



# Prolonged post-differentiation culture influences the expression and biophysics of Na<sup>+</sup> and Ca<sup>2+</sup> channels in induced pluripotent stem cell-derived ventricular-like cardiomyocytes

Gracious R. Ross<sup>1</sup> · Farhan Rizvi<sup>1</sup> · Larisa Emelyanova<sup>1</sup> · A. Jamil Tajik<sup>2</sup> · Arshad Jahangir<sup>2</sup>

Received: 9 November 2018 / Accepted: 4 April 2019 / Published online: 30 April 2019  
© Springer-Verlag GmbH Germany, part of Springer Nature 2019

## Abstract

Several studies have been reported in various domains from induction methods to utilities of somatic cell pluripotent reprogramming. However, one of the major struggles facing the research field of induced pluripotent stem cell (iPSC)-derived target cells is the lack of consistency in observations. This could be due to variety of reasons including varied culture periods post-differentiation. The cardiomyocytes (CMs) derived from iPSCs are commonly studied and proposed to be utilized in the comprehensive in vitro proarrhythmia initiative for drug safety screening. As the influence of varied culture periods on the electrophysiological properties of iPSC-CMs is not clearly known, using whole-cell patch clamp technique, we compared two groups of differentiated ventricular-like iPSC-CMs that are cultured for 10 to 15 days (D10–15) and more than 30 days ( $\geq$  D30) both under current and voltage clamps. The prolonged culture imparts increased excitability with high-frequency spontaneous action potentials, robust increase in the magnitude of peak Na<sup>+</sup> current density, relatively shallow inactivation kinetics of Na<sup>+</sup> channels, faster recovery from inactivation, and augmented Ca<sup>2+</sup> current density. Quantitative real-time PCR studies of  $\alpha$ -subunit transcripts showed enhanced mRNA expression of *SCN1A*, *SCN5A* Na<sup>+</sup> channel subtypes, and *CACNA1C*, *CACNA1G*, and *CACNA1I* Ca<sup>2+</sup> channel subtypes, in  $\geq$  D30 group. Conclusively, the prolonged culture of differentiated iPSC-CMs affects the excitability, single-cell electrophysiological properties, and ion channel expressions. Therefore, following standard periods of culture across research studies while utilizing ventricular-like iPSC-CMs for in vitro health/disease modeling to study cellular functional mechanisms or test high-throughput drugs' efficacy and toxicity becomes crucial.

**Keywords** iPSC · Cardiomyocyte · Channels · Electrophysiology

## Introduction

Since the seminal discovery of the reprogramming to pluripotency in somatic cells (Takahashi et al. 2007; Takahashi and Yamanaka 2006; Yu et al. 2007), myriad studies have been reported in variety of domains like methods of pluripotency induction, differentiation, maturation to target cell type, and utilities in terms of cell therapy, organ culture, precision medicine, and in vitro physiology/pathology modeling to

study cellular functional mechanisms or high-throughput testing of drugs' efficacy and toxicity. However, as increasing number of labs adopt induced pluripotent stem cell (iPSC)-derived target cells, a major struggle facing the iPSC research field is the lack of consistency in observations (Scudellari 2016). One of the commonly studied promising cell type is the cardiomyocytes (CMs) derived from iPSCs. It is also proposed to utilize human iPSC-CM in the comprehensive in vitro proarrhythmia initiative for drug safety screening (Gintant et al. 2017). However, these iPSC-derived CMs (iPSC-CMs) are generally considered to be immature both developmentally and electrophysiologically (Uosaki et al. 2015; Veerman et al. 2015; Zuppinger et al. 2017) (Sinnecker et al. 2014). In cardiac cell clusters derived from even human embryonic stem cells, variability of action potentials is reported both within and among the cell clusters (Zhu et al. 2016). Moreover, the varied post-differentiation culture periods followed in biochemical assays and functional experiments in iPSC-CM (Ma et al. 2011; Moreau et al. 2017)

✉ Gracious R. Ross  
gracious.ross@aurora.org

<sup>1</sup> Center for Integrative Research on Cardiovascular Aging, Aurora Research Institute, Aurora Health Care, 2900 W Oklahoma Ave, Milwaukee, WI 53215, USA

<sup>2</sup> Aurora Cardiovascular Services, Aurora Sinai/St. Luke's Medical Centers, Milwaukee, WI, USA

can also influence the overall consistency and reproducibility of the studies. Although most of the reported iPSC-CMs start evincing spontaneous action potentials (“beating”) from day 3 following differentiation, it is challenging to use them in critical efficacy, safety, and mechanistic studies without knowing the period in which stability and fidelity of the biophysical properties of ion channels are attained. Temporal changes in phenotype of human iPSC-CMs are evident in an earlier study (Ivashchenko et al. 2013). Because the influence of varied culture periods on the electrophysiological properties of iPSC-derived ventricular-like CMs is not clearly known, we compared the electrophysiological properties of two groups of differentiated ventricular-like iPSC-CMs that are in post-differentiation culture for 10 to 15 days (D10–15) and more than 30 days ( $\geq$  D30). We report here that prolonged culture imparts a robust increase in the magnitude of  $\text{Na}^+$  currents, faster recovery from inactivation without any change in the activation-inactivation kinetics, enhanced mRNA expression of *SCN1A* and *SCN5A* channel subtypes accompanied by augmented  $\text{Ca}^{2+}$  current density, and elevated gene expression of *CACNA1C*, *CACNA1G*, and *CACNA1I* channels.

## Material and methods

**Cells** The iPSC-CMs were received as a gift from the Center for Integrated Research on Cardiovascular Aging (CIRCA) of Aurora Research Institute, Milwaukee, WI. About the generation of cells, briefly, Sendai virus reprogrammed human cardiac fibroblast-derived iPSCs from ATCC, Manassas, VA, were maintained in Geltrex® matrix-coated six-well plates in Essential 8 Flex medium. On day 0, iPSCs were treated with GSK3 selective inhibitor CHIR99021 and medium was changed on day 2. On day 3, cells were treated with another small molecule IWR-1 (WNT inhibitor) to direct iPSC to a cardiac lineage. By day 10, majority of iPSC were differentiated into beating cardiomyocytes and were grown in RPMI-B27 without insulin for the next 3 weeks. The cells were screened routinely for the presence and/or absence of lineage markers. The differentiated cardiomyocytes were characterized by the presence of sarcomeric  $\alpha$ -actinin, troponin 1, and Cx43 assessed by expression, immunostaining, and flow cytometry.

**General electrophysiology** Standard patch clamp technique was used in this study (Hamill et al. 1981). Action potentials and ionic currents were recorded from single iPSC-CM with whole-cell patch clamp technique, under current clamp and voltage clamp configurations, respectively, at room temperature, using EPC 10 patch clamp amplifier (HEKA, Lambrecht/Pfalz, Germany) and patch micropipettes with resistances of 3 to 5 M $\Omega$  (Sutter Instruments Company, Novato, CA). Series resistance and cell capacitance were compensated to between

50 and 80% in all voltage clamp recordings. For spontaneous action potential recordings under current clamp, iPSC-CMs were held in zero input current and voltage changes were recorded continuously.  $\text{Na}^+$  currents were recorded by holding the cell at  $-90$  mV followed by depolarizing potentials in 10 mV increment. Extracellular bath solution perfusion was continuous using gravity with solution exchange requiring  $\sim 1$  min. All the experiments were performed under HEPES-buffered external solution containing the following (in mM): NaCl, 150; KCl, 5.4;  $\text{CaCl}_2$ , 1.8;  $\text{MgCl}_2$ , 1; glucose, 15; HEPES, 15; Na-pyruvate, 1 (pH 7.4 (NaOH)); and patch pipette solution containing the following (in mM): KCl, 150; NaCl, 5;  $\text{CaCl}_2$ , 2; EGTA, 5; HEPES, 10; MgATP, 5 (pH 7.2 (KOH)). Steady-state inactivation of  $\text{Na}^+$  currents was measured using two-step voltage protocols (prepulse from  $-120$  to  $+40$  mV for 100 ms at an increment of 10 mV and a test pulse of  $-50$  mV for 300 ms), whereas voltage dependence of activation was calculated from peak current-voltage relationships assuming a reversal potential of  $+40$  mV. The time course of recovery from inactivation of  $\text{Na}^+$  channels was studied using a double-pulse protocol in which two identical voltage clamp pulses were delivered from a holding potential ( $V_h$ ) of  $-90$  mV to a step potential of  $-50$  mV for 100 ms with increasing interpulse interval (10 ms increment) at 0.2 Hz.  $\text{Ca}^{2+}$  currents were recorded at  $V_h$  of  $-40$  mV followed by depolarizing potentials in 10 mV increment.

**Data acquisition and analysis** Signals were filtered at 5–10 kHz (3 dB, four-pole Bessel) and digitized at 10–100  $\mu\text{s}$ . Patchmaster data files were converted to axon binary file (ABF) formats using the ABF Utility program (Synaptosoft, Fort Lee, NJ) and were analyzed by Clampfit 10.1 (Molecular Devices, Sunnyvale, CA) or Igor Pro 6.0 (WaveMetrics, Portland, OR). Nonlinear and linear curve fittings were performed with Clampfit while Boltzmann fits were performed either in Clampfit or GraphPad Prism (La Jolla, CA). Conductance-voltage curves were calculated from the peak current according to the equation ( $G_{\text{Na}} = I_{\text{Na}}/(V - E_{\text{Na}})$ ) where  $V$  is the test pulse potential and  $E_{\text{Na}}$  the reversal potential extrapolated from the current ( $I$ )-voltage ( $V$ ) relationship. The activation curves ( $G$ - $V$ ) were fitted using the Boltzmann function  $G/G_{\text{max}} = 1/\{1 + \exp[(V - V_{1/2})/k]\}$ , where  $G/G_{\text{max}}$  is the normalized  $\text{Na}^+$  conductance,  $V_{1/2}$  is the potential of half-maximum activation, and  $k$  is the slope factor. Data fittings with exponential functions,  $I = \sum A_i \exp(-t/\tau_i) + C$ , were carried out using Clampfit. Data are presented as the means and SE of  $n$  observations.  $P < 0.05$  was considered significant (unpaired  $t$  test).

**Real-time PCR of  $\text{Na}_v\text{-}\alpha$  and  $\text{Ca}_v\text{-}\alpha$  subunit genes** Total RNA was isolated from iPSC-CMs using Trizol Reagent (Thermo Fisher Scientific, Waltham, MA) according to the manufacturer’s instructions. RNA concentrations were

evaluated spectrophotometrically using the NanoQuant on the Tecan Infinite M200 plate reader (Tecan Group, Mannedorf, Switzerland). Total RNA (500 ng) was used for reverse transcription using the miScript RT II kit with the supplied HiFlex buffer (Qiagen, Valencia, CA). Quantitative (q) PCR was performed on the LightCycler®480 II System (Roche, Pleasanton; CA) in a total reaction volume of 25  $\mu$ l/well in LightCycler® Multiwell 96, white reaction plate, using the predesign TaqMan® Assay 5'-FAM reporter and 3'-MGB quencher (Thermo Fischer Scientific, Waltham, CA) for the following primers: SCN1A (Hs00374696), SCN2A (Hs01109871), SCN3A (Hs00366902), SCN4A (Hs001109480), SCN5A (Hs00165693), SCN8A (Hs00274075), SCN9A (Hs01076699), SCN10A (Hs01045137), SCN11A (Hs00204222), CACNA1C (Hs00167681), CACNA1G (Hs00367969), and CACNA1I (Hs01096207); (Part No. 4453320) using TaqMan® Universal Master mix (Thermo Fischer Scientific, Waltham, CA) and 10 ng diluted cDNA per well with GAPDH (Hs02786624) (TaqMan® assay reagent) served as internal control. The amplification conditions were 95 °C for 10 min, followed by 40 cycles of 95 °C for 15 s, 60 °C for 1 min, 72 °C for 40s, and 1 cycle of 65 °C for 1 min, 97 °C continuous, and 40 °C for 30 s. Data were normalized against GAPDH reference gene and differences in the values of steady-state levels of mRNA were calculated (Pfaffl 2001). Fold change was calculated by taking the ratio of  $\geq$  D30 to D10–15.

## Results and discussion

The major findings of this study are that prolonged post-differentiation culture of iPSC-CMs causes changes in the following single-cell electrophysiological properties and channel expressions: (1) relatively high frequency of spontaneous APs; (2) robust increase in the Na<sup>+</sup> currents; (3) relatively shallow inactivation kinetics of Na<sup>+</sup> channels; (4) faster recovery from inactivation of Na<sup>+</sup> channels; (5) significant increase in the expression of Na<sub>v</sub>1.1 and Na<sub>v</sub>1.5 channel subtypes; (6) enhanced Ca<sup>2+</sup> current density; and (7) augmented expression of Ca<sub>v</sub>1.2, Ca<sub>v</sub>3.1, and Ca<sub>v</sub>3.3 channel subtypes.

### Action potential properties

The effect of prolonged culture post-differentiation on the excitability of ventricular-like iPSC-CMs was determined by analyzing the spontaneous AP recordings under current clamp. The AP parameters such as the interval(s), maximal diastolic potential (MDP, mV), peak (mV), amplitude (peak-to-peak magnitude, mV), maximum rise slope (dV/dt, V/s), and durations measured at various percent levels of re-polarization amplitudes [action

potential duration (APD)<sub>10</sub>, APD<sub>30</sub>, APD<sub>40</sub>, APD<sub>70</sub>, APD<sub>80</sub>, APD<sub>90</sub>] were measured and analyzed between the two groups: D10–15 and  $\geq$  D30. Only the iPSC-CMs with APs that had a ratio of greater than 1.5 in APD<sub>30–40</sub>/APD<sub>70–80</sub> (Ma et al. 2011) were considered ventricular-like. Prolonged culture significantly ( $P < 0.05$ ) reduced the interval between spontaneous AP (D10–15:  $15 \pm 6$  s ( $n = 4$ ) vs  $\geq$  D30:  $7 \pm 2$  s ( $n = 11$ )) and relatively depolarized maximum diastolic potential (D10–15:  $-69 \pm 3$  mV ( $n = 4$ ) vs  $\geq$  D30:  $-59 \pm 4$  mV ( $n = 11$ )) without any effect on all other AP parameters (Fig. 1). Therefore, the primary effect of prolonged culture is an increased frequency of spontaneous firing, indicating an enhanced excitability of iPSC-CMs. A range of values for MDP and beats per minute of human ventricular-like iPSC-CM APs have been reported earlier from  $-57$  to  $-75$  mV and 28 to 72, respectively (Hoekstra et al. 2012; Itzhaki et al. 2011; Ma et al. 2011). Our observations of MDP fall within this range but the interval between APs are quite long in the D10–15 group. Prolonged culture has relatively depolarized the MDP by  $\sim 10$  mV, which although appears to have no significant role in the excitability of the iPSC-CMs as the frequency of AP generation is significantly increased, probably that the repolarization is hyperpolarized—enough to recover the Na<sup>+</sup> channels from inactivation.

### Voltage dependence and activation/inactivation kinetics of Na<sup>+</sup> channels

Human iPSC-CMs express Na<sup>+</sup> channels (Moreau et al. 2017), which are important to generate a cardiac AP (Morad and Tung 1982). The cardiac Na<sup>+</sup> current contributes to the AP upstroke in ventricular cardiomyocytes (Berecki et al. 2010). Therefore, we analyzed the biophysical characteristics of Na<sup>+</sup> channels to determine the changes, if any, caused by prolonged culture. Na<sup>+</sup> currents were recorded under voltage clamp from a  $V_h$  of  $-90$  mV with depolarizing test pulses (500 ms) stepped at a 10-mV increment (Fig. 2a). The current-voltage relationship of Na<sup>+</sup> currents (Fig. 2b) showed significantly higher magnitude of peak currents normalized to cell capacitance (D10–15:  $-17 \pm 8$  pA/pF,  $n = 4$ ;  $\geq$  D30:  $-130 \pm 42$  pA/pF,  $n = 5$ ), without any shift in the voltage dependence of activation in  $\geq$  D30 group cells. The mean capacitances were not significantly different between D10–15 ( $36 \pm 9$  pF) and  $\geq$  D30 ( $49 \pm 9$  pF). The membrane excitability is also influenced by voltage-dependent activation and steady-state inactivation of Na<sup>+</sup> channels (Amaya et al. 2006). Steady-state inactivation of Na<sup>+</sup> currents was measured using two-step voltage protocols as represented in Fig. 2c. The voltage dependence of activation and inactivation in both D10–15 and  $\geq$  D30 groups was measured as described in the methods and fit by the Boltzmann function to determine the voltage ( $V_{1/2}$ ) for half-maximal activation or inactivation and the corresponding slope factors (Fig. 2d). The values of  $V_{1/2}$  of activation of Na<sup>+</sup> channels were not significantly different after prolonged culture [ $-59 \pm 4$  mV,  $k = 3 \pm 2$  (D10–15),  $n = 3$ ;  $-$

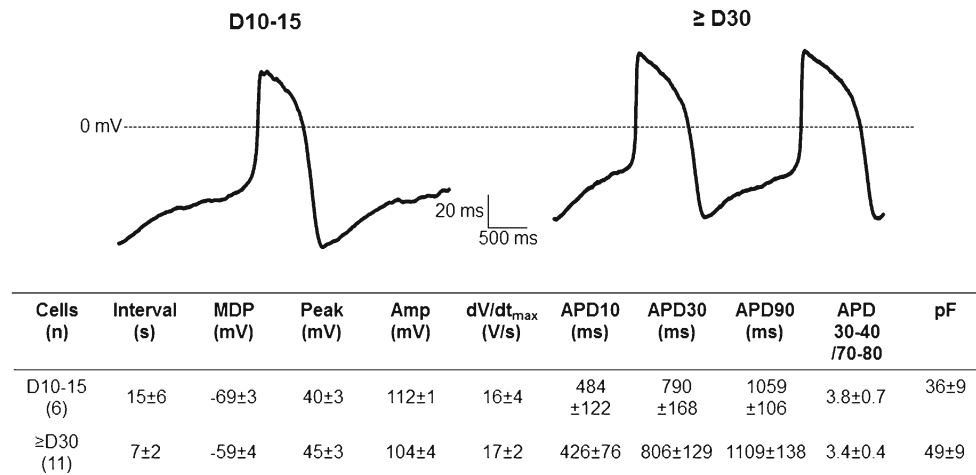


**Fig. 1** Action potentials (APs) were recorded from human induced pluripotent stem cell-derived ventricular-like cardiomyocytes (iPSC-CM) at room temperature under whole-cell configuration of patch clamp method. Refer text for details. Representative current clamp recordings of spontaneous APs from iPSC-CMs cultured for 10 to

15 days (D10–15; left) and for more than 30 days (≥D30; right). Bottom table lists the different AP parameters between the two groups. Interval: beat rate interval; MDP: maximum diastolic potential; Peak: peak voltage; Amp: amplitude; dV/dt<sub>max</sub>: maximal rate of depolarization; APD: AP duration at different levels of repolarization

57 ± 2 mV,  $k = 2 ± 1$  (≥D30),  $n = 5$ ] while the values of  $V_{1/2}$  of inactivation were  $-62 ± 2$  mV,  $k = 8 ± 2$  in D10–15 ( $n = 3$ ) and

$-66 ± 1$  mV,  $k = 4 ± 1$  in the ≥D30 groups ( $n = 5$ ). The corresponding slope factors ( $k$ ) of activation and inactivation of Na<sup>+</sup>

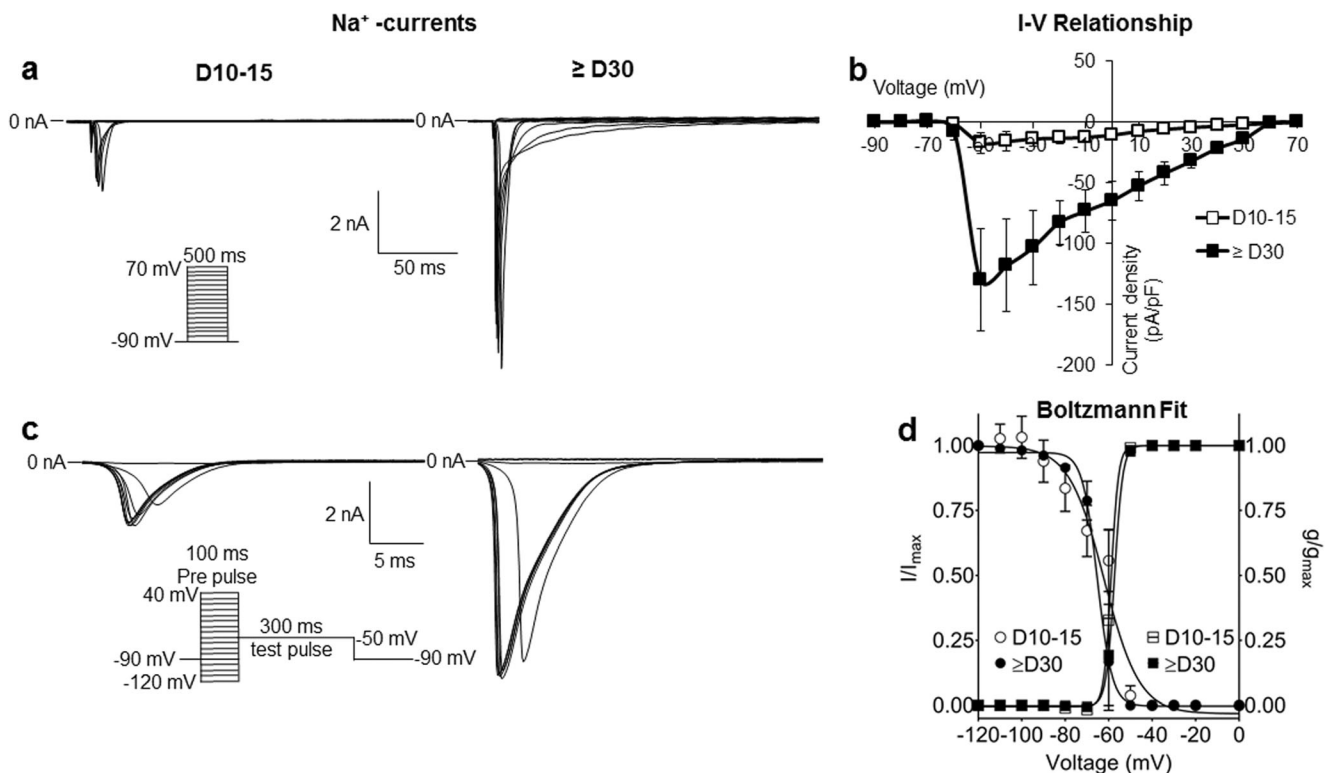


**Fig. 2** **a** Representative Na<sup>+</sup> current ( $I_{Na}$ ) traces were elicited by the voltage protocol as shown in the inset (left) in both D10–15 (left) and ≥D30 (right) groups. **b** Graph depicts the current-voltage relationship with significantly higher peak  $I_{Na}$  density (normalized to cell capacitance) in the ≥D30 group. **c** Representative recordings of steady-state inactivation of Na<sup>+</sup> currents that were measured using two-step voltage protocols (inset bottom left: prepulse from  $-120$  to  $+40$  mV for 100 ms at an increment of 10 mV and a test pulse of  $-50$  mV for

300 ms) in both D10–15 (left) and ≥D30 (right) groups. **d** Voltage dependence of steady-state activation and inactivation of Na<sup>+</sup> currents. Normalized peak conductance (squares) and steady-state inactivation curves (circles) of Na<sup>+</sup> currents are shown. The curves were fit by Boltzmann function to determine the voltage ( $V_{1/2}$ ) for half-maximal activation or inactivation and the corresponding slope factors. Data are expressed as means ± SE ( $n = 3–5$ ), analyzed by unpaired Student's  $t$  test

channels in D10–15 and  $\geq$ D30 groups showed a shallow slope for inactivation after prolonged culture. Prolonged culture did not significantly affect the activation kinetics of  $\text{Na}^+$  channels compared with the D10–15 group while relatively slowed down the inactivation kinetics. The time-dependent increase in the expression of the  $\text{Na}^+$  current is similar to previous reports in stem cell-derived cardiomyocytes from mice (Malan et al. 2011) and humans (Barbuti and Robinson 2015; Ivashchenko et al. 2013; Sheng et al. 2012). Interestingly, the  $dV/dt_{\text{max}}$  of APs was not different between the two groups although the  $\text{Na}^+$  current density is high following prolonged culture. This could be due to similar functional availability of  $\text{Na}^+$  channels at the time of AP generation between the groups. Single-channel studies may be required to determine the actual functional availability of these channels (Ross et al. 2010).

### Recovery of $\text{Na}^+$ channels from inactivation

We analyzed the recovery of  $\text{Na}^+$  channels from inactivation using a paired-pulse protocol as illustrated in Fig. 3a, bottom. Identical clamp pulses ( $P_1$ ,  $P_2$ ) were delivered from a  $V_h$  of  $-90$  mV to a step potential of  $-50$  mV with a variable interpulse interval (10-ms increment,  $P_1$ – $P_2$ ) at 0.2 Hz. The current during  $P_2$  ( $I_2$ ) relative to the current during  $P_1$  ( $I_1$ ) was plotted as a function of the  $P_1$ – $P_2$  reactivation interval ( $\Delta t$ ) as shown in Fig. 3b. Monoexponential function was applied to fit the reactivation curves to assess the reactivation time constants. Prolonged culture significantly hastened the recovery with a faster recovery time constants (15 ms [95% CI, 14–17 ms,  $n = 5$ ]) of  $\text{Na}^+$  channels from inactivation compared with the D10–15 group (74 ms [95% CI, 65–83 ms,  $n = 3$ ]). Therefore, the generation of high-frequency spontaneous APs and hyper-excitability could be due to faster recovery rate of  $\text{Na}^+$  channels from inactivation states after prolonged culture. The delay in the recovery from inactivation of  $\text{Na}^+$  channels in

the D10–15 group could probably be due to a lower fraction of  $\text{Na}^+$  channels having entered inactivated states (slow inactivation) causing slower recovery (Blair and Bean 2003).

### Gene expression of $\text{Na}^+$ channel subtypes

Enhanced  $\text{Na}^+$  current magnitude and increased frequency spontaneous APs following prolonged culture could be due to increased expression of  $\text{Na}^+$  channels. Several subtypes of voltage-dependent  $\text{Na}^+$  channels are expressed in human iPSC-CMs (Moreau et al. 2017). Therefore, we measured the changes in mRNA expression, if any, induced by prolonged culture post-differentiation, using quantitative real-time PCR technique. Transcripts of  $\text{Na}^+$  channel  $\alpha$ -subunit subtypes, including  $\text{Na}_v1.1$  (*SCN1A*),  $\text{Na}_v1.2$  (*SCN2A*),  $\text{Na}_v1.3$  (*SCN3A*),  $\text{Na}_v1.4$  (*SCN4A*),  $\text{Na}_v1.5$  (*SCN5A*),  $\text{Na}_v1.6$  (*SCN8A*),  $\text{Na}_v1.7$  (*SCN9A*),  $\text{Na}_v1.8$  (*SCN10A*), and  $\text{Na}_v1.9$  (*SCN11A*), were detected and analyzed in iPSC-CMs from both D10–15 and  $\geq$ D30 groups. Cardiac  $\text{Na}^+$  current is mediated by voltage-gated sodium channels composed of the pore-forming alpha-subunits and the accessory beta-subunits. Various  $\text{Na}^+$  channel alpha-subunits are variably expressed in the mammalian heart with differential responsiveness to various pharmacological agents (Catterall 2012; Sakakibara et al. 1992). While the  $\text{Na}_v1.5$  is the most expressed subunit in the human heart representing the bulk of the  $\text{Na}^+$  channels (DeMarco and Clancy 2016), diverse subtypes of voltage-dependent  $\text{N}^+$  channels are reported to be expressed in human iPSC-CMs (8). As depicted in Fig. 4, there was a 7.5- and 38-fold increase in *SCN1A* and *SCN5A* channel subtypes at mRNA level, respectively, following prolonged culture. The differences observed in the frequency of spontaneous APs, magnitude of  $\text{Na}^+$  currents, and recovery of  $\text{Na}^+$  channels from inactivation in iPSC-

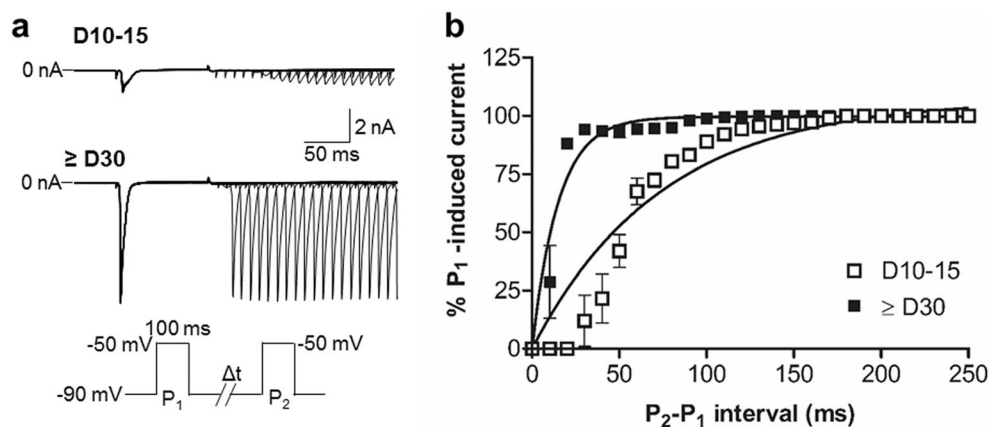


**Fig. 3** Recovery from inactivation of  $\text{Na}^+$  channels. **a** Superimposed typical tracings of  $\text{Na}^+$  current recovery in ventricular-like iPSC-CM from D10–15 (top) and  $\geq$ D30 (bottom) groups. Voltage protocol is shown in bottom inset as  $P_1$  and  $P_2$ , identical pulses delivered at varying  $P_1$  and  $P_2$  interval ( $\Delta t$ ). **b**  $P_2$  current normalized to  $P_1$  current

and plotted vs  $P_1$ – $P_2$  interval ( $\Delta t$ ). The reactivation curves were fitted with a monoexponential function of the form  $I = A \exp(-t/\tau)$ . Prolonged culture ( $\geq$ D30; filled squares) hastened the recovery rate (15 ms) of  $\text{Na}^+$  channels from inactivation in relation to D10–15 groups (74 ms). Data are expressed as means  $\pm$  SE ( $n = 3$ –5, unpaired Student's *t* test)

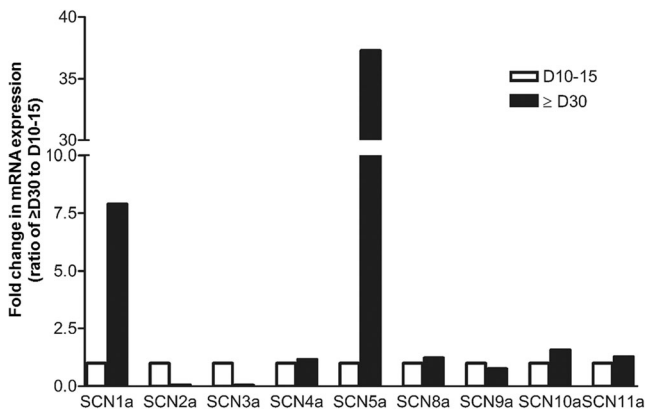


**Fig. 4** Quantitative analysis of mRNA expression of Na<sup>+</sup> channel subtypes by real-time PCR. Analysis of transcripts of  $\alpha$ -subunits of Na<sup>+</sup> channels [Na<sub>v</sub>1.1 (*SCN1A*), Na<sub>v</sub>1.2 (*SCN2A*), Na<sub>v</sub>1.3 (*SCN3A*), Na<sub>v</sub>1.4 (*SCN4A*), Na<sub>v</sub>1.5 (*SCN5A*), Na<sub>v</sub>1.6 (*SCN8A*), Na<sub>v</sub>1.7 (*SCN9A*), Na<sub>v</sub>1.8 (*SCN10A*), and Na<sub>v</sub>1.9 (*SCN11A*)] in iPSC-CMs from D10–15 and  $\geq$  D30 groups, showed significant fold increase in Na<sub>v</sub>1.1 (7.5-fold) and Na<sub>v</sub>1.5 (38-fold) channel subtypes in the  $\geq$ D30 group. The mRNA expression  $\alpha$ -subunits of Na<sup>+</sup> channels were normalized to GAPDH and fold changes were calculated by taking the ratio of  $\geq$ D30 to D10–15 days

CMs of  $\geq$ D30 group following prolonged culture could be related to increased expression of Na<sub>v</sub>1.1 and Na<sub>v</sub>1.5 channel subtypes. Auxiliary subunits have also been shown to influence the biophysical processes of activation and inactivation of Na<sup>+</sup> channels and oligomerization of individual channels, in addition to modulate gating and regulate expression (DeMarco and Clancy 2016; Moreau et al. 2017; Patton et al. 1994). More studies are required to determine the influence of prolonged culture, if any, over the expression of auxiliary subunits of Na<sup>+</sup> channels.

### Changes in Ca<sup>2+</sup> currents

The importance of Ca<sup>2+</sup> to the function of heart was discovered over 120 years ago by Sydney Ringer when he found that the heart would not beat if Ca<sup>2+</sup> was absent (Ringer 1883). Ca<sup>2+</sup> is also proven to be the link between excitation and cardiac contractility that starts during the upstroke of the AP leading to L-type Ca<sup>2+</sup> channel opening (Bodi et al. 2005; Nerbonne and Kass 2005). Therefore, we determined the effect of prolonged culture on the whole-cell Ca<sup>2+</sup> currents in human iPSC-CMs. After confirming that the cells are ventricular-like based on their respective action potentials under current clamp, Ca<sup>2+</sup> currents were recorded under voltage clamp from a  $V_h$  of  $-40$  mV with depolarizing test pulses (500 ms) stepped at a 10-mV increment up to  $+50$  mV (Fig. 5a). Earlier reports have demonstrated the presence of L-type Ca<sup>2+</sup> currents in human iPSC-CM with varied biophysical characteristics including peak current density, across studies (Ivashchenko et al. 2013; Ma et al. 2011; Yazawa et al. 2011). In our study,

the current-voltage relationship of Ca<sup>2+</sup> currents (Fig. 5b) showed significantly higher magnitude of peak currents normalized to cell capacitance (D10–15:  $-3 \pm 1$  pA/pF,  $n = 4$ ;  $\geq$  D30:  $-6 \pm 1$  pA/pF,  $n = 6$ ,  $P = 0.04$ ) in  $\geq$ D30 group cells, without any shift in the voltage dependence of activation. The control peak current density is in accordance with the previous report of 3.3 pA/pF by Yazawa et al. (2011), while much lower from another study (Ma et al. 2011). Our observations fall within the reported amplitudes of the maximal current density in human isolated native ventricular cardiomyocytes that range from 2.2 to 10.2 pA/pF (Hoekstra et al. 2012; Magyar et al. 2000; Mewes and Ravens 1994). The variations across iPSC-CM studies could be due to different experimental conditions related to temperature, extracellular Ca<sup>2+</sup> concentration, intracellular Ca<sup>2+</sup> buffering, etc., making absolute comparisons less feasible. Enhanced Ca<sup>2+</sup> current magnitude following prolonged culture could be due to increased expression of Ca<sup>2+</sup> channels. Therefore, we also determined the effect of prolonged culture on the gene expression levels of  $\alpha$ -subunits of Ca<sup>2+</sup> channel subtypes including Ca<sub>v</sub>1.2 (*CACNA1C*), Ca<sub>v</sub>3.1 (*CACNA1G*), and Ca<sub>v</sub>3.3 (*CACNA1I*). As depicted in Fig. 5c, following prolonged culture ( $\geq$  D30), there was a significant fold (0.5 to 2) increase in gene expression of Ca<sub>v</sub>1.2, Ca<sub>v</sub>3.1, and Ca<sub>v</sub>3.3 channel subtypes. Ca<sub>v</sub>1.2 encoded by *CACNA1C* genes constitute the alpha-subunit of the  $I_{CaL}$ , whereas *CACNA1G* and *CACNA1H* genes encode for the Ca<sub>v</sub>3.1 and Ca<sub>v</sub>3.3 subunits that form the transient Ca<sup>2+</sup> current ( $I_{CaT}$ ). Even though the transcripts for  $\alpha$ -subunits of T-type Ca<sup>2+</sup> channels are also detected in this study, we did not see any clear functional activity of these channels in iPSC-CMs between the voltage range of  $-70$  to  $-50$  mV, in concordance with earlier reports (Ma et al. 2011), while another study detected small T-type currents in about 8% of cells on day 37 and 50% of cells on day 45 (Ivashchenko et al. 2013) which probably may be non-ventricular-like cells. In human native ventricular cardiomyocytes, T-type Ca<sup>2+</sup> channels are reported to be functionally absent in health and become functionally expressed only in pathological conditions (Ono and Iijima 2010).

Taken together, prolonged post-differentiation culture of human ventricular-like iPSC-CMs affects the excitability, single-cell electrophysiological properties, and ion channel expressions. At which period of culture, the biophysical characteristics of ion channels become stable, and thereby, steady excitability requires a longer temporal study. Moreover, culture periods affect pharmacological responsiveness (Ivashchenko et al. 2013), which is highly likely due to these altered ion channel electrophysiology. Therefore, following standard periods of post-differentiation culture across research studies while utilizing ventricular-like iPSC-CMs for in vitro health/disease modeling to study

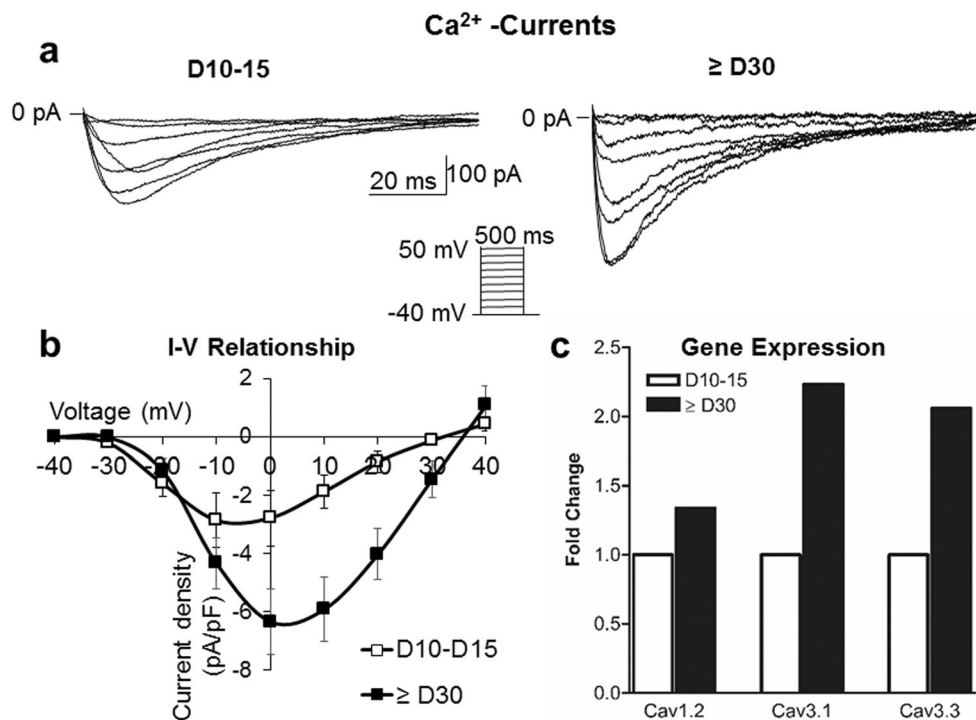


**Fig. 5** **a** Representative  $\text{Ca}^{2+}$  current ( $I_{\text{Ca}}$ ) traces were elicited by the voltage protocol as shown in the inset in both D10–15 (left) and  $\geq$ D30 (right) groups. **b** Graph depicts the current-voltage relationship with significantly higher peak  $I_{\text{Ca}}$  density (normalized to cell capacitance) in the  $\geq$ D30 group. Data are expressed as means  $\pm$  SE ( $n=3$ , unpaired  $t$  test). **c** Quantitative analysis of transcripts of  $\alpha$ -subunits of  $\text{Ca}^{2+}$  channels

[ $\text{Ca}_v1.2$  (*CACNA1C*),  $\text{Ca}_v3.1$  (*CACNA1G*), and  $\text{Ca}_v3.3$  (*CACNA1D*)] in iPSC-CMs from D10–15 and  $\geq$ D30 groups, showed significant fold increase in  $\text{Ca}_v1.2$  (0.5-fold),  $\text{Ca}_v3.1$  (2-fold), and  $\text{Ca}_v3.3$  (2-fold) channel subtypes in the  $\geq$ D30 group. The mRNA expression  $\alpha$ -subunits of  $\text{Ca}^{2+}$  channels were normalized to GAPDH and fold changes were calculated by taking the ratio of  $\geq$ D30 to D10–15 days

cellular functional mechanisms or test high-throughput drugs' efficacy and toxicity becomes crucial.

### Study limitations

In this study, two post-differentiation culture periods of human ventricular-like iPSC-CMs were selected based on some of the earlier reports (Ma et al. 2011; Moreau et al. 2017). We observed spontaneous action potentials, which are usually associated with an immature phenotype, even in the  $\geq$ D30 group. Therefore, further studies with longer post-differentiation culture periods may be required to determine when spontaneous action potentials cease, to assess whether this is due to immature phenotype or innate characteristic of iPSC-derived ventricular-like cardiomyocytes.

**Acknowledgements** The authors are thankful to Dr. Rosy Joshi-Mukherjee, Research Scientist, Center for Integrated Research on Cardiovascular Aging (CIRCA) of Aurora Research Institute, for the generous gift of iPSC-CMs, and Stacie Edwards for maintenance of cells and qPCR data acquisition.

**Authors' contribution** GR conceptualized and designed the work, acquired and interpreted the patch clamp data, and wrote the manuscript. FR, LE, AJT, and AJ interpreted the data and critically revised the manuscript for important intellectual content.

### Compliance with ethical standards

**Conflict of interest** The authors declare that there is no conflict of interest.

### References

- Amaya F, Wang H, Costigan M, Allchorne AJ, Hatcher JP, Egerton J, Stean T, Morisset V, Grose D, Gunthorpe MJ, Chessell IP, Tate S, Green PJ, Woolf CJ (2006) The voltage-gated sodium channel  $\text{Na}(v)1.9$  is an effector of peripheral inflammatory pain hypersensitivity. *J Neurosci* 26:12852–12860
- Barbuti A, Robinson RB (2015) Stem cell-derived nodal-like cardiomyocytes as a novel pharmacologic tool: insights from sinoatrial node development and function. *Pharmacol Rev* 67:368–388
- Berecki G, Wilders R, de Jonge B, van Ginneken AC, Verkerk AO (2010) Re-evaluation of the action potential upstroke velocity as a measure of the  $\text{Na}^+$  current in cardiac myocytes at physiological conditions. *PLoS One* 5:e15772
- Blair NT, Bean BP (2003) Role of tetrodotoxin-resistant  $\text{Na}^+$  current slow inactivation in adaptation of action potential firing in small-diameter dorsal root ganglion neurons. *J Neurosci* 23:10338–10350
- Bodi I, Mikala G, Koch SE, Akhter SA, Schwartz A (2005) The L-type calcium channel in the heart: the beat goes on. *J Clin Invest* 115:3306–3317
- Catterall WA (2012) Voltage-gated sodium channels at 60: structure, function and pathophysiology. *J Physiol* 590:2577–2589
- DeMarco KR, Clancy CE (2016) Cardiac Na channels: Structure to Function. *Curr Top Membr* 78:287–311

- Gintang G, Fermini B, Stockbridge N, Strauss D (2017) The evolving roles of human iPSC-derived cardiomyocytes in drug safety and discovery. *Cell Stem Cell* 21:14–17
- Hamill OP, Marty A, Neher E, Sakmann B, Sigworth FJ (1981) Improved patch-clamp techniques for high-resolution current recording from cells and cell-free membrane patches. *Pflugers Arch* 391:85–100
- Hoekstra M, Mummery CL, Wilde AA, Bezzina CR, Verkerk AO (2012) Induced pluripotent stem cell derived cardiomyocytes as models for cardiac arrhythmias. *Front Physiol* 3:346
- Itzhaki I, Maizels L, Huber I, Zwi-Dantsis L, Caspi O, Winterstern A, Feldman O, Gepstein A, Arbel G, Hammerman H, Boulos M, Gepstein L (2011) Modelling the long QT syndrome with induced pluripotent stem cells. *Nature* 471:225–229
- Ivashchenko CY, Pipes GC, Lozinskaya IM, Lin Z, Xiaoping X, Needle S, Grygielko ET, Hu E, Toomey JR, Lepore JJ, Willette RN (2013) Human-induced pluripotent stem cell-derived cardiomyocytes exhibit temporal changes in phenotype. *Am J Physiol Heart Circ Physiol* 305:H913–H922
- Ma J, Guo L, Fiene SJ, Anson BD, Thomson JA, Kamp TJ, Kolaja KL, Swanson BJ, January CT (2011) High purity human-induced pluripotent stem cell-derived cardiomyocytes: electrophysiological properties of action potentials and ionic currents. *Am J Physiol Heart Circ Physiol* 301:H2006–H2017
- Magyar J, Iost N, Kortvely A, Banyasz T, Virag L, Szigligeti P, Varro A, Opincariu M, Szecsi J, Papp JG, Nanasi PP (2000) Effects of endothelin-1 on calcium and potassium currents in undiseased human ventricular myocytes. *Pflugers Arch* 441:144–149
- Malan D, Friedrichs S, Fleischmann BK, Sasse P (2011) Cardiomyocytes obtained from induced pluripotent stem cells with long-QT syndrome 3 recapitulate typical disease-specific features in vitro. *Circ Res* 109:841–847
- Mewes T, Ravens U (1994) L-type calcium currents of human myocytes from ventricle of non-failing and failing hearts and from atrium. *J Mol Cell Cardiol* 26:1307–1320
- Morad M, Tung L (1982) Ionic events responsible for the cardiac resting and action potential. *Am J Cardiol* 49:584–594
- Moreau A, Mercier A, Theriault O, Boutjdir M, Burger B, Keller DI, Chahine M (2017) Biophysical, molecular, and pharmacological characterization of voltage-dependent sodium channels from induced pluripotent stem cell-derived cardiomyocytes. *Can J Cardiol* 33:269–278
- Nerbonne JM, Kass RS (2005) Molecular physiology of cardiac repolarization. *Physiol Rev* 85:1205–1253
- Ono K, Iijima T (2010) Cardiac T-type Ca(2+) channels in the heart. *J Mol Cell Cardiol* 48:65–70
- Patton DE, Isom LL, Catterall WA, Goldin AL (1994) The adult rat brain beta 1 subunit modifies activation and inactivation gating of multiple sodium channel alpha subunits. *J Biol Chem* 269:17649–17655
- Pfaffl MW (2001) A new mathematical model for relative quantification in real-time RT-PCR. *Nucleic Acids Res* 29:e45
- Ringer S (1883) A further contribution regarding the influence of the different constituents of the blood on the contraction of the heart. *J Physiol* 4:29–42 23
- Ross GR, Kang M, Akbarali HI (2010) Colonic inflammation alters Src kinase-dependent gating properties of single Ca<sup>2+</sup> channels via tyrosine nitration. *Am J Physiol Gastrointest Liver Physiol* 298:G976–G984
- Sakakibara Y, Wasserstrom JA, Furukawa T, Jia H, Arentzen CE, Hartz RS, Singer DH (1992) Characterization of the sodium current in single human atrial myocytes. *Circ Res* 71:535–546
- Scudellari M (2016) A decade of iPSC cells. *Nature* 534:310–312
- Sheng X, Reppel M, Nguemo F, Mohammad FI, Kuzmenkin A, Hescheler J, Pfannkuche K (2012) Human pluripotent stem cell-derived cardiomyocytes: response to TTX and lidocaine reveals strong cell to cell variability. *PLoS One* 7:e45963
- Sinnecker D, Laugwitz KL, Moretti A (2014) Induced pluripotent stem cell-derived cardiomyocytes for drug development and toxicity testing. *Pharmacol Ther* 143:246–252
- Takahashi K, Tanabe K, Ohnuki M, Narita M, Ichisaka T, Tomoda K, Yamanaka S (2007) Induction of pluripotent stem cells from adult human fibroblasts by defined factors. *Cell* 131:861–872
- Takahashi K, Yamanaka S (2006) Induction of pluripotent stem cells from mouse embryonic and adult fibroblast cultures by defined factors. *Cell* 126:663–676
- Uosaki H, Cahan P, Lee DI, Wang S, Miyamoto M, Fernandez L, Kass DA, Kwon C (2015) Transcriptional landscape of cardiomyocyte maturation. *Cell Rep* 13:1705–1716
- Veerman CC, Kosmidis G, Mummery CL, Casini S, Verkerk AO, Bellin M (2015) Immaturity of human stem-cell-derived cardiomyocytes in culture: fatal flaw or soluble problem? *Stem Cells Dev* 24:1035–1052
- Yazawa M, Hsueh B, Jia X, Pasca AM, Bernstein JA, Hallmayer J, Dolmetsch RE (2011) Using induced pluripotent stem cells to investigate cardiac phenotypes in Timothy syndrome. *Nature* 471:230–234
- Yu J, Vodyanik MA, Smuga-Otto K, Antosiewicz-Bourget J, Frane JL, Tian S, Nie J, Jonsdottir GA, Ruotti V, Stewart R, Slukvin II, Thomson JA (2007) Induced pluripotent stem cell lines derived from human somatic cells. *Science* 318:1917–1920
- Zhu R, Millrod MA, Zambidis ET, Tung L (2016) Variability of action potentials within and among cardiac cell clusters derived from human embryonic stem cells. *Sci Rep* 6:18544
- Zuppinger C, Gibbons G, Dutta-Passecker P, Segiser A, Most H, Suter TM (2017) Characterization of cytoskeleton features and maturation status of cultured human iPSC-derived cardiomyocytes. *Eur J Histochem* 61:2763

**Publisher's note** Springer Nature remains neutral with regard to jurisdictional claims in published maps and institutional affiliations.